# CHAPTER 4

## Results and Discussions

### 4.1 Substrate Material

As seen in Figure 4.1, the structure of as-received DSS observed under SEM show elongated coarse microstructure. The darker image is the ferrite phase while the lighter image is the austenite islands of DSS. The grains are oriented parallel to the rolling direction which formed during extrusion production process. The hardness of DSS with coarse microstructure before boronizing process was 350 Hv.

In order for the DSS to become superplastic material, it was solution treated and cold rolled to have single ferrite phase and large elongated grains as shown in Figure 4.2. The initial hardness of the fine microstructure DSS before boronizing was 445 Hv which is higher than coarse microstructure DSS. The increase in hardness for the fine microstructure was due to cold working effect where the strain hardening occurred inside the grains.

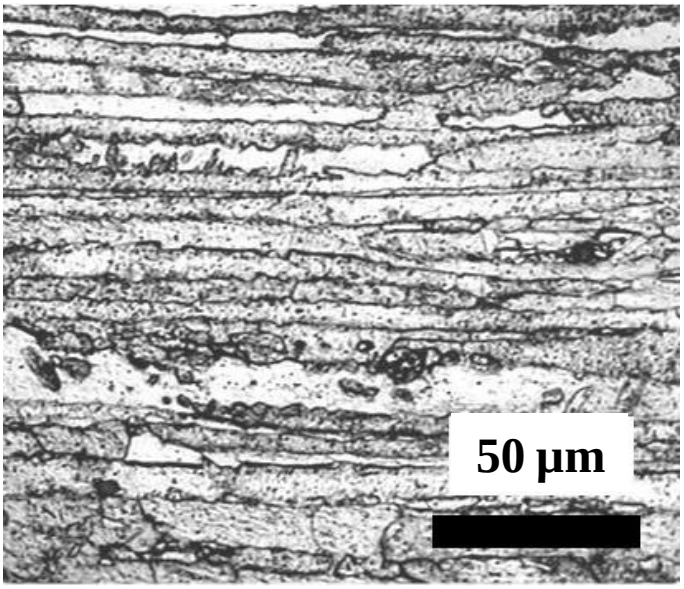


Figure 4.1 SEM image of microstructure of the coarse DSS

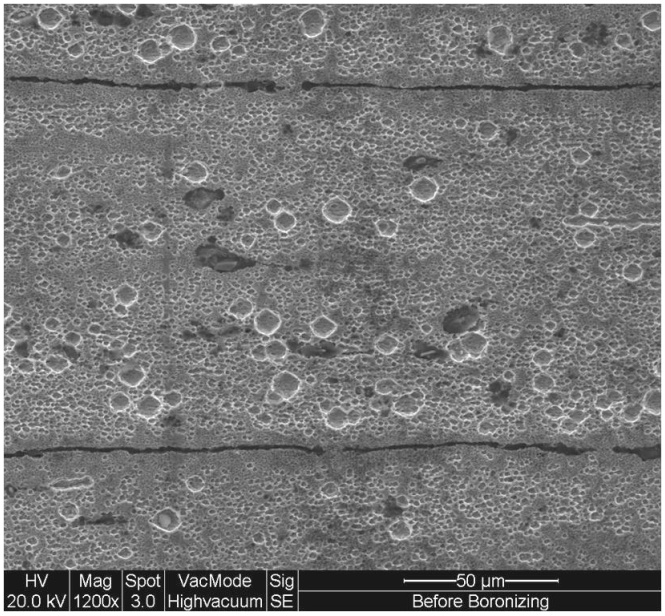


(a)

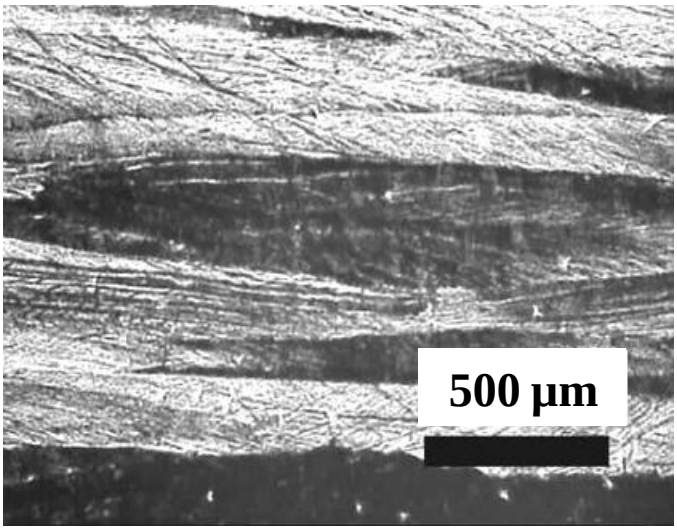


(b)

Figure 4.2 DSS microstructure after solution treated at 1573 K for 1 hour, water quenched and cold rolled up to 75%. (a) SEM image, (b) Optical micrograph

## 4.2 Superplastic Boronizing

Figure 4.3 illustrate the appearance of specimen before and after SPB through compression test at 0.2 strains. The specimen can be superplastically compressed without crack until 0.6 strains. Figure 4.4 shows the microstructure of a specimen after compression for 0.6 strains at 1223 K at $2\times10^{-4}$ $s^{-1}$ strain rate, which yielded fine grains duplex microstructure with an average size of approximately 3 μm.

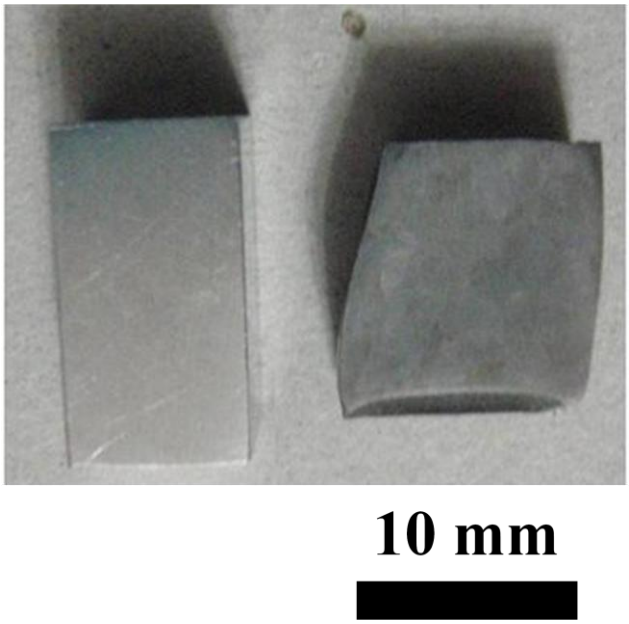


Figure 4.3 Side view of specimen before (left) and after (right) SPB at compressive strain of 0.2 at temperature 1223 K

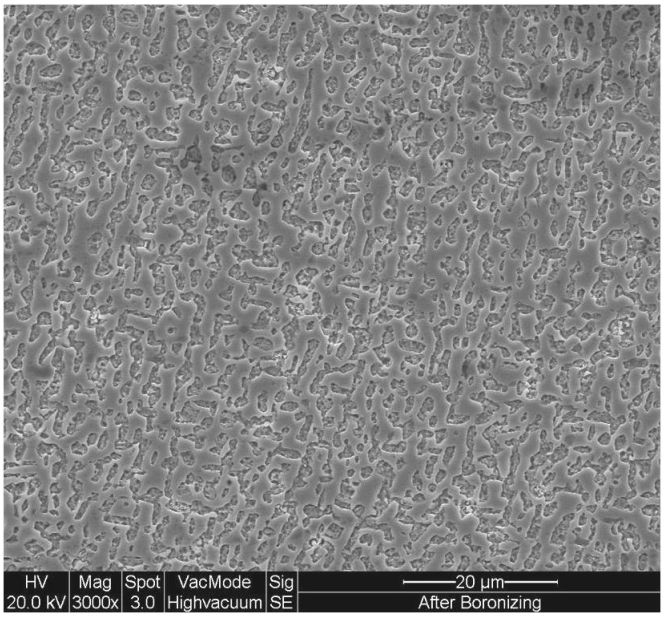


Figure 4.4 Microstructure of a specimen after compression for 0.6 strains at 1223 K at $2 \times 10^{-4}\ s^{-1}$ strain rate.

### 4.2.1 XRD Analysis

XRD analysis was carried out to confirm the existence of borides at the diffusion layer. XRD pattern of boronized layer on the surface of DSS boronized at 1273 K and 0.6 strains given in Figure 4.5 shows various peaks of FeB, $Fe_2B$, CrB, $CrB_4$ and $Ni_3B$.

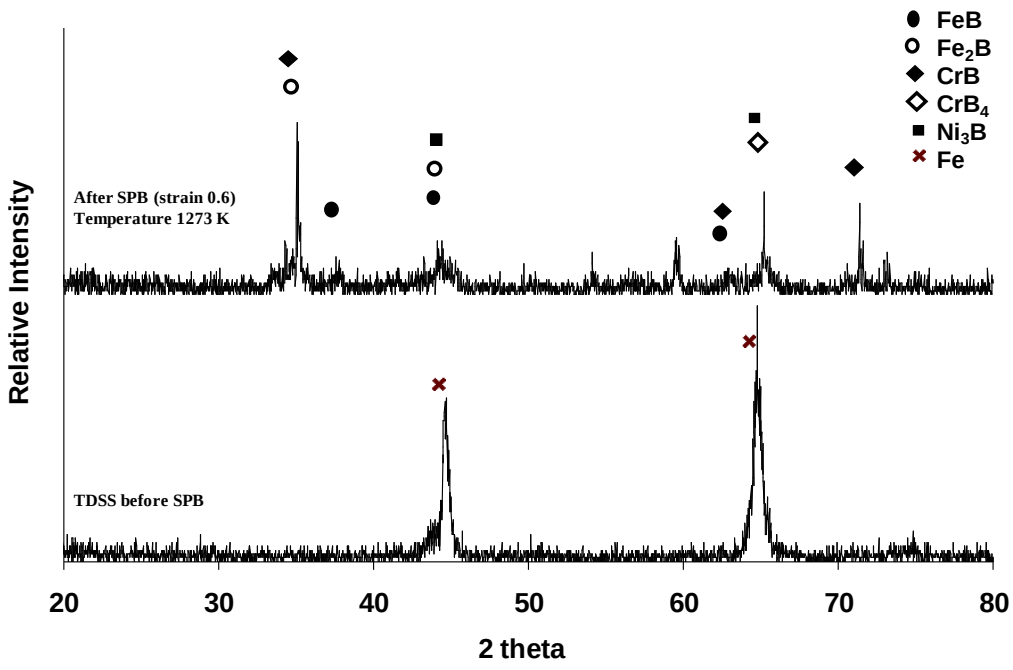


Figure 4.5 The XRD patterns of DSS before and after boronizing

### 4.2.2 Flow Stress Behaviour

Figure 4.6 shows a typical set of stress strain relation of specimens deformed at three different temperatures at 0.4 strains. In the initial stage of the deformation, DSS exhibit linear behavior characterized by a shallow slope that reflects the increase in stress necessary to deform the material. As the deformation march on, the flow stress rises to a maximum then drop to the steady state reveal on the stress-strain curve indicating a flow hardening at the commencement of the strain and a flow softening after a certain degree of strain. Finally, the curve again displays a positive slope at high strain region.

Through the literature reported by Seshacharyulu (2000), the curves all exhibit continuous dynamic recrystallization (DRX) characteristic that stress increases to peak followed by softening, and then remain constant. The DRX characteristic of the stress is cause by microstructural evolution of work hardening, DRX occurrence and steady state. As such, flow stress behavior reveals in Figure 4.6 shows that superplasticity in this case arises from local strain hardening and the subsequent recrystallization. The downward deflection of the work-hardening rate derives from the nucleation of new unstrained grains and represents the onset of dynamic recrystallization.

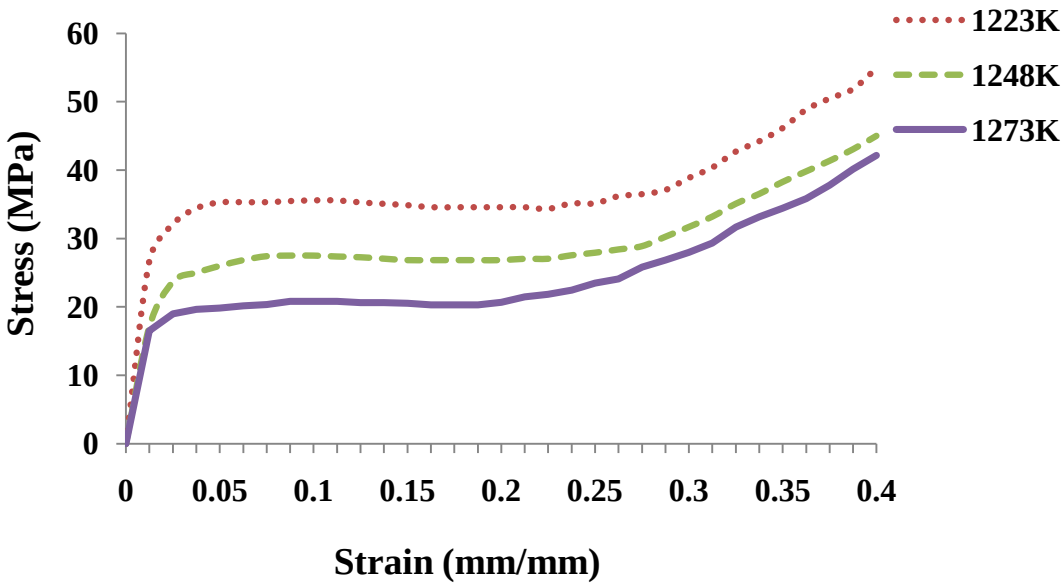


Figure 4.6 Stress strain relation of specimens at 0.4 strains

From Figure 4.6, the higher the temperature the lower the flow stresses. At high temperatures, the material's response can be characterized by low peak strains and stresses, with the steady state obtained relatively fast. A decrease in temperature results

in increases in peak stress and peak strain. In this case, much higher strains are required to reach a steady state condition, indicating a reduction in the dynamic recrystallization rate. This is well consistent with the result that the higher deformation temperature the easier the occurrence of DRX. This is because diffusion increases with the increases of temperature and thus DRX occurs more easily. However, in general the flow stresses of all specimens are considerably low. Deformation of superplastic DSS at temperature 1223 K under compression produced a low stress of only about 50 MPa.

### 4.2.3 Microstructure of Boronized Layer

Figure 4.7 show the optical images of cross-sectional DSS microstructures superplastically boronized at different temperature condition. Optical image illustrate boronized layer formed on the steel surface have smooth and compact morphology. This was due to high alloying elements in DSS. It was reported that alloying elements especially chromium and nickel modify coating-substrate interface by changing the diffusivity of boron atoms (Ozbek et al., 2002; Ozbek et al., 2004). Therefore, the morphology becomes more compact and smoother as the alloying elements are higher.

The thickness of boronized layer formed range from 10.7 μm to 29.0 μm and was mainly dependent on the temperature and time. Higher temperature shows thicker layer thickness. Boronized layer of DSS deformed at 0.4 strains was in the range of 15.7 μm to 25.1 μm at different temperature. Superplastic deformation occurs mainly from the mechanism of grain boundary sliding with accommodation of either diffusion, slip of fine grains or both. These same grains were to have been transporting the boron

atoms from the surface to the inner part of the substrate through the said grain boundary sliding and slipping. While boronizing temperature increase, diffusion rate of boron was speeded up. Therefore, thicker boronized layer was achieved at higher boronizing temperature.

Figure 4.8 shows the boronized layer at different strain conditions with 1273 K. At this temperature, boronized layer thickness increase from 17.5 μm to 24.4 μm with increasing strain from 0.2 to 0.6. Table 4.1 and Figure 4.9 summarize the boronized layer thickness for superplastically boronized DSS obtained at every condition in this study and the time required.

Previous study on CB showed that boronized layer thickness of 19 μm was obtained after boronizing at 1223 K for one hour (Hasan, 2005), which is equivalent to boronizing time of 3600 seconds. SPB at same temperature, under $2 \times 10^{-4}$ $s^{-1}$ strain rate shows that at strain 0.6 or equivalent to 3000 seconds, 17.3 μm of boronized layer was obtained. Boronized layer thickness produced by SPB for 3600 seconds at 1223 K is estimated 19.1 μm by using the chart show in Figure 4.13. SPB seems report similar thickness of boronized layer to that of CB. It should be noted that, the boronizing powder thickness in SPB is very thin as compare to CB. Studies show that to produce good boronized material, a certain powder thickness is necessary to ensure enough supply of boron source to the substrate. The layer thickness of iron boride, as well as the associated mass gain depends on the surface boron concentration related to the boron powder thickness. For instance, Jain and Sundararajan (2002) discovered decrease in the thickness of boronized layer at low pack thickness. Lesser amount of boron source in the pack probably restrained the boronized layer growth in this study.

Besides, short deformation time, 50 minutes, could be a reason of similar boron penetration was observed in present study compare to CB. From previous research (Hasan, 2005), it is noticeable boronized layer thickness increment show by SPB is comparatively apparent at longer boronizing time.

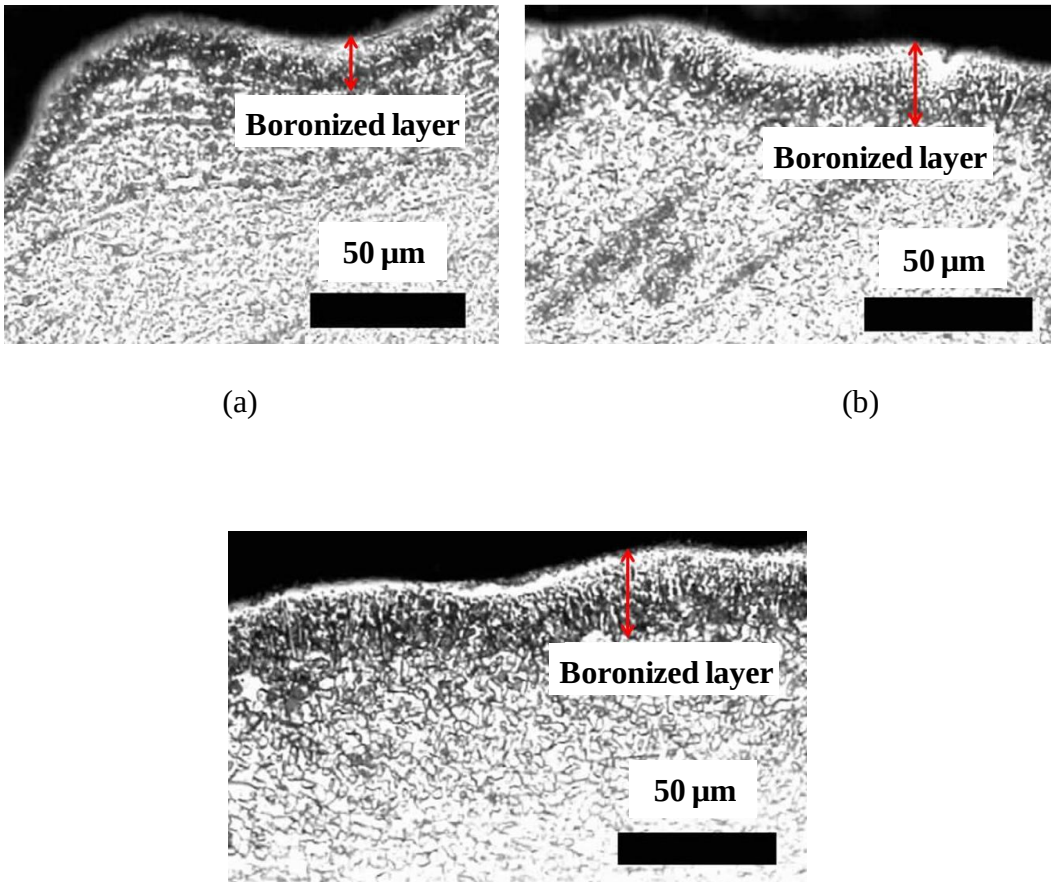


(a) (b)

(c)

Figure 4.7 Cross section images of SPB specimens at three different temperatures. (0.4 strains); (a) $T_1$ = 1223 K, (b) $T_2$ = 1273 K, (c) $T_3$ = 1323 K

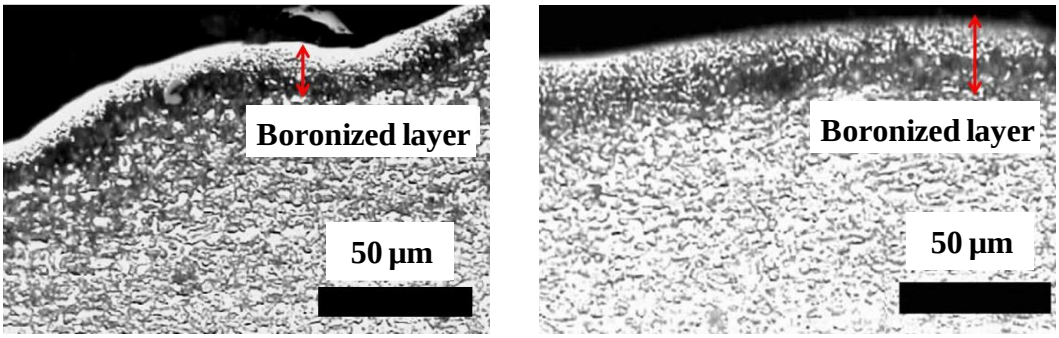


(a) (b)

Figure 4.8 Cross section images of SPB specimens at two different strains under 1273 K. (a) strain = 0.2, (b) strain = 0.6

Table 4.1 Boronized layer thickness and surface hardness for SPB with a strain rate of $2 \times 10^{-4}\ s^{-1}$, at various temperatures and strains

| Temperature (K) | Time (s) | Strain | Boronized layer (µm) | Hardness (Hv) |
|---|---|---|---|---|
| 1223 | 1000 | 0.2 | 10.7 | 949.8 |
| | 2000 | 0.4 | 15.7 | 1241.0 |
| | 3000 | 0.6 | 17.3 | 1252.5 |
| 1273 | 1000 | 0.2 | 17.5 | 1234.5 |
| | 2000 | 0.4 | 21.2 | 1447.5 |
| | 3000 | 0.6 | 24.4 | 1607.5 |
| 1323 | 1000 | 0.2 | 20.4 | 1291.1 |
| | 2000 | 0.4 | 25.1 | 1572.0 |
| | 3000 | 0.6 | 29.0 | 1687.7 |

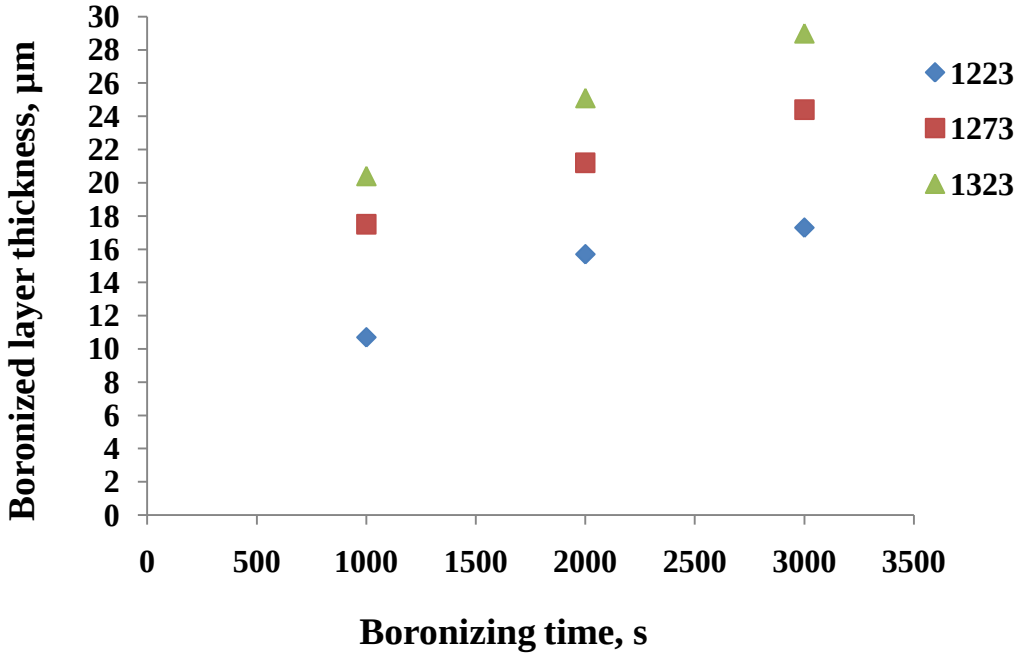


Figure 4.9 The variation of boronized layer thickness with boronizing time and temperature for superplastically boronized DSS

### 4.2.4 Hardness Profile

Figure 4.10 shows boronized surface hardness profiles of superplastically boronized DSS. Depending on boronizing time and temperature, the surface hardness values were about 1687.7 Hv to 302.7 Hv from the surface to the core. The gradient of surface hardness was confirmed by microhardness of cross-sectioned specimen as shown in Figure 4.10 and 4.12. The hardness of the boronized layer is much higher than that of the substrate because of the presence of hard FeB, $Fe_2B$ and chromium boride phases. Figure 4.11 show higher degree of deformation results a better mechanical property represented by hardness gradient. This is because higher strain not only allows

more superplastic deformation to occur, but also allows for more boronizing time exposure. Superplastic deformation also creates high densities of vacancies, dislocation and subgrain boundaries was believed has increase the diffusion rate of atoms.

The surface hardness for CB at 1223 K and 3600 seconds was approximately 1250 Hv (Hasan, 2005), which did not show significant different from the value obtained by SPB (1252.5 Hv) along with a shorter boronizing time (3000 seconds) at the same temperature.

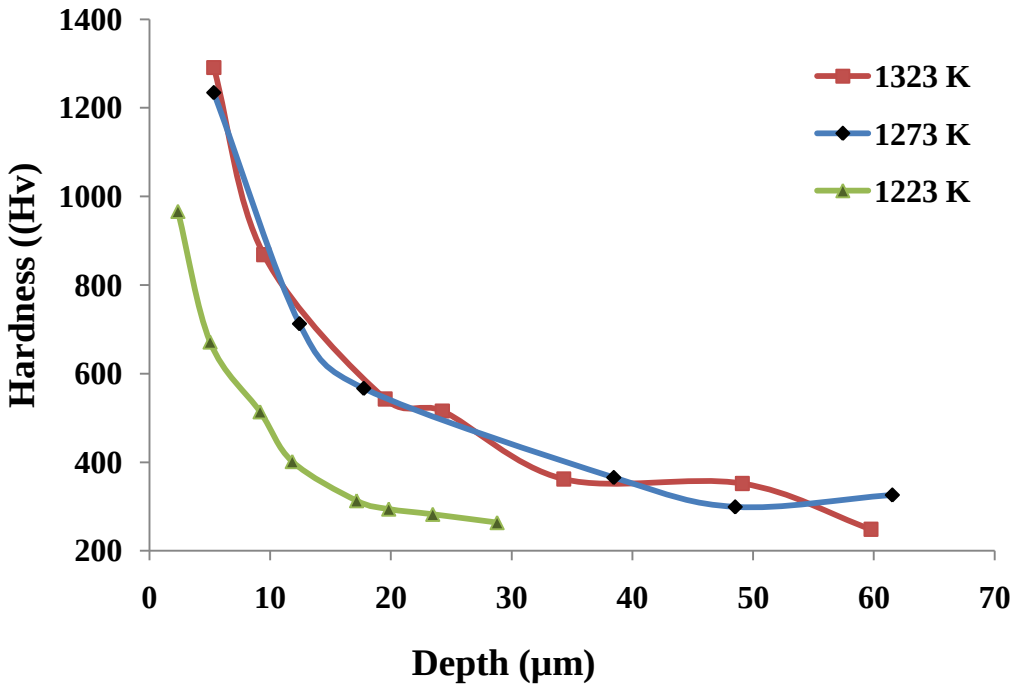


Figure 4.10 Hardness gradient of cross-sectioned specimens deformed at strain 0.2

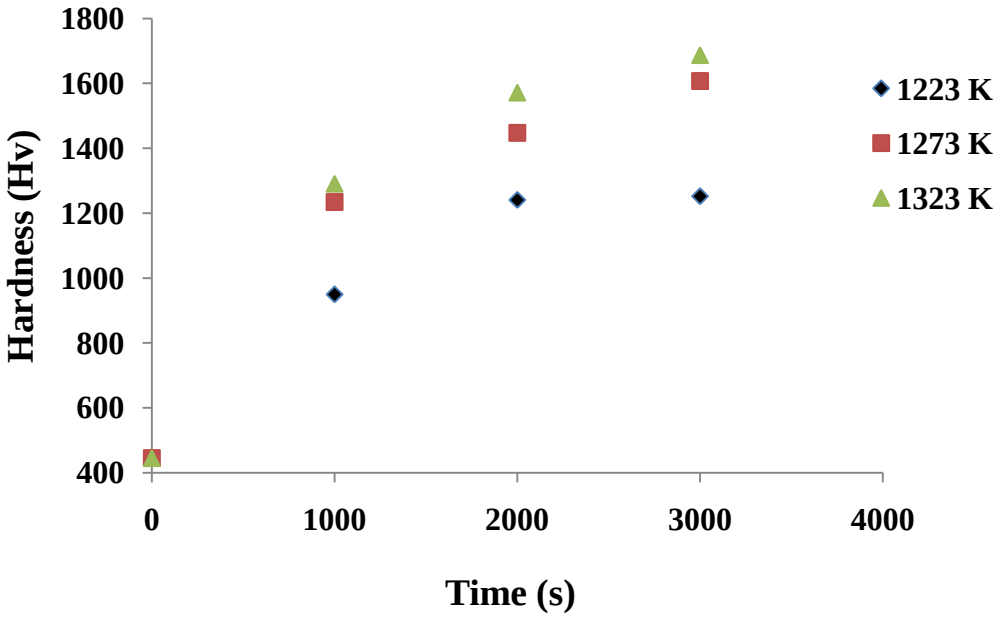


Figure 4.11 Surface hardness profiles

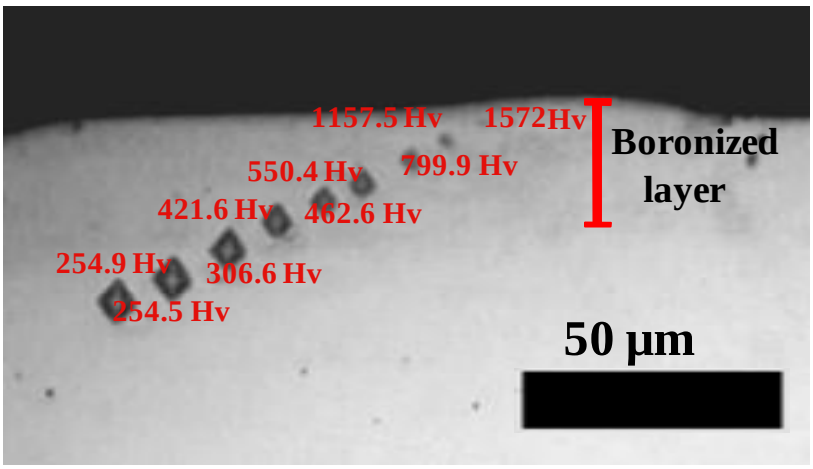


Figure 4.12 Microhardness profile measured on sectioned surface of superplastically boronized DSS for 2000 seconds at 1323 K

### 4.2.5 Activation Energy Analysis

In this study, the effects of strain (time) and temperature on the growth kinetics of the boronized layer were investigated. According to Sen et al. (2005a), the growth rate of boronized layer is controlled by boron diffusion in the FeB, $Fe_2B$ sublayers, and boronized layer growth occurs because of boron diffusion perpendicular to the surface of the specimen. Therefore, the activation energy of boronizing process can be determined using the thickness of boronized layer formed.

As shown in Figure 4.9 above, the depth of boronized layer thickness varies with time and follows the well-known parabolic law (Chen and Wang, 1999; Genel et al., 2003; Sen et al., 2005a; Sen et al., 2005b) as follows:

$$d^2 = Kt \qquad (4.1)$$

where $d$ is the boronized layer thickness (μm), $t$ is boronizing time (s) and $K$ is boron growth rate constant or diffusion coefficient of boron into boronized layer. As mentioned earlier, boronized layer growth, rely mainly on the diffusion of boron atoms into the FeB and $Fe_2B$ sublayers. Figure 4.13 indicates that the square of boronized layer thickness progresses linearly with time for the periods between 1000 and 3000 seconds.

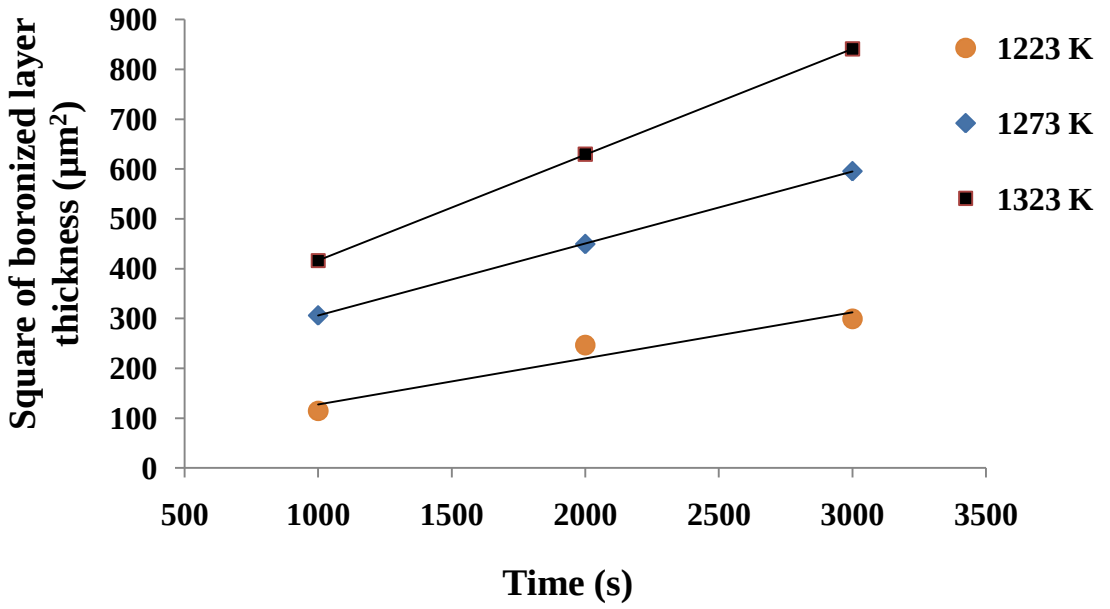


Figure 4.13 Square of boronized layer thickness versus boronizing time

The relationship between the diffusion coefficients, $K$ ($m^2$ $s^{-1}$), activation energy, $Q$ (J $mol^{-1}$) and boronizing temperature, $T$ (K) can be expressed by an Arrhenius equation as follows:

$$K = K_o e^{-\left(\frac{Q}{RT}\right)} \tag{4.2}$$

where $K_o$ is the pre-exponential constant and $R$ is the gas constant (8.314 J $mol^{-1}$ $K^{-1}$). Taking the natural logarithm of Equation (4.2), Equation (4.3) can be derived as follows:

$$\ln K = \ln K_o + \left(-QR^{-1}\right)\left(T^{-1}\right) \tag{4.3}$$

As shown in Figure 4.14, the plot of ln $K$ versus reciprocal boronizing temperature ($T^{-1}$) is linear. The slope of straight line will determine the activation energy ($Q$) of the boronizing process. The results show that $K$ increases with boronizing temperature. The $K$ values ranged from $9.2 \times 10^{-14}$ $m^2$ $s^{-1}$ to $2.1 \times 10^{-13}$ $m^2$ $s^{-1}$. The activation energy ($Q$) for boronizing process of microstructure DSS was determined as 111 kJ $mol^{-1}$ and the pre-exponential constant ($K_o$) was $5.1 \times 10^{-9}$ $m^2$ $s^{-1}$.

However, through previous study result, activation energy of conventional boronized DSS was known as 192.1 kJ $mol^{-1}$ (Hasan, 2005), which is higher than superplastic boronized DSS of present study. Activation energy reduce by 81.1 kJ $mol^{-1}$ (~42.2%) is achieved. Thus, we can conclude that SPB reduced the energy required for boron atoms to diffuse into DSS. Time and temperature are the critical parameters for both conventional and SPB process.

In addition, superplastic boronized DSS at 1223 K show higher diffusion coefficients, $K$, $9.2 \times 10^{-14}$ $m^2$ $s^{-1}$ compare to that of conventional boronized DSS at same temperature, $5.44 \times 10^{-14}$ $m^2$ $s^{-1}$. In conventional method, the self and grain boundary diffusion is expected to be the mechanism controlling the process. Meanwhile, superplastic deformation occurs mainly from the grain boundary sliding and slipping of the fine grain is widely known. Faster diffusion rate of boron into the substrate was obtained through grain boundary sliding and slipping.

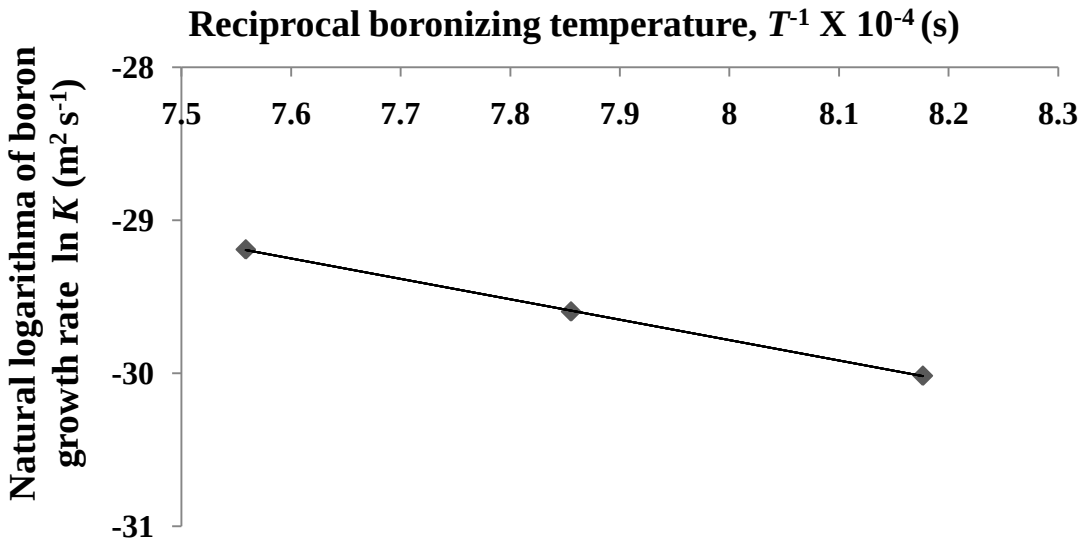


Figure 4.14 Natural logarithm of boron growth rate (ln $K$) $m^2s^{-1}$ versus reciprocal boronizing temperature ($T^{-1}$) s for superplastically boronized DSS

### 4.2.6 Powder Consumption

Table 4.2 shows the usage of boronizing compound for both the conventional and SPB process. Note that the amount of boronizing powder used for SPB process was only 10 g. CB process used 37.7 g boron powder, about 3.8 times of powder consumption of SPB process. Moreover, the whole specimen of CB process is embedded inside the powder surroundings of 13 mm thickness. The pack thickness of the boron powder around the superplastically boronizing DSS surface is 5 mm, about 62% lower than pack thickness of CB. Even though the powder usage for superplastic process was lesser than that of CB process, it is still sufficient to form a boronized layer with similar quality with respect to surface hardness and boronizing layer thickness.

SPB method is more economical and suitable to be used in the applications that only require boronizing one site surface of specimen. High cost of boronizing process has limited its applications. Highly reduce the amount of boron powder consumption bring down the cost of the boronizing process. Almost 73% of the boron powder can be saved through the SPB process compared to the CB method without sacrificing the boronized layer properties. Therefore, this new surface hardening technique should be strongly considered and implemented in the surface engineering area.

Table 4.2 Boronizing powder amount in conventional and superplastic boronizing of DSS

| Process | Description | Number of boronized surface | Boronizing powder amount |
|---|---|---|---|
| Conventional boronizing | Powder pack method with the whole specimen is embedded inside the powder surroundings of 13 mm thickness. | Six | 37.7 g |
| Superplastic boronizing | One surface of the specimen is placed on the powder with 5 mm thickness. Different compression load is applied on top of the specimen. | One | 10.0 g |